sciendo

TRANSACTIONS ON AEROSPACE RESEARCH
1(258) 2020, pp.1-17
DOI: 10.2478/tar-2020-0001
eISSN 2545-2835

PERFORMANCE OF QUIET HELICOPTER

Jarosław Stanisławski
Łukasiewicz Research Network – Institute of Aviation
Al. Krakowska 110/114, 02-256 Warsaw, Poland
jaroslaw.stanislawski@ilot.edu.pl • ORCID: 0000-0003-1629-4632

Abstract

Noise generated by helicopters is one of the main problems associated with the operation of rotorcrafts. Requirements for reduction of helicopter noise were reflected in the regulations introducing lower limits of acceptable rotorcraft noise. A significant source of noise generated by helicopters are the main rotor and tail rotor blades. Radical noise reduction can be obtained by slowing down the blade tips speed of main and tail rotors. Reducing the rotational speed of the blades may decrease rotor thrust and diminish helicopter performance. The problem can be solved by attaching more blades to main rotor. The paper presents results of calculation regarding improvement of the helicopter performance which can be achieved for reduced rotor speed but with increased number of rotor blades. The calculations were performed for data of hypothetical light helicopter. Results of simulation include rotor loads and blade deformations in chosen flight conditions. Equations of motion of flexible rotor blades were solved using the Galerkin method which takes into account selected eigen modes of the blades. The simulation analyzes can help to determine the performance and loads of a quiet helicopter with reduced rotor speed within the operational envelope of helicopter flight states.

Keywords: helicopter, noise, rotor loads.

1. INTRODUCTION

Envelope of helicopter operations which include the flight states from hover to high speed flight enables performing wide range of civil and military tasks. Especially in search, rescue and emergency service helicopters are useful, but with growing number of flights the harmful effects of helicopter noise can be noticed. In USA in narrow region of the Grand Canyon more than 300 air tour helicopters fly the area each day [1]. Community of the Hawaiian Islands also complains about excessive helicopter noise [2]. Arising protests of population of large cities against noise generated by helicopters gave impulse to introduce more stringent certification regulations as well to develop modern quieter helicopters [3]. Helicopter noise certification procedures and limitations of allowable noise level due to mass of helicopter are formulated in ICAO (International Civil Aviation Organization) Annex 16 Volume1 Chapter 8 [4] which is applicable to all helicopter types and in Chapter 11 which provides simplified certification procedure for light helicopters with a maximum take-off mass up to 3,175kg. Helicopter noise limits for take-off according to ICAO Annex 16 Chapter8 and noise levels for some helicopter types confirmed during EASA (European Aviation Safety Agency) certification [5] are compared in Fig.1. The blades of main rotor are the main source of helicopter noise. The main rotor generates primarily noise which is

made up of basic loading noise and broadband turbulence noise. Additionally in descent flight Blade Vortex Interaction (BVI) noise can be generated and at high forward speed High Speed Impulsive (HSI) noise occurs. Large efforts were focused on development the efficient methods for predicting the rotorcraft noise which were verified basing on flight test data [6], [7]. NASA applied noise prediction method consisting of a rotorcraft comprehensive analysis (CAMRAD II) computing helicopter trim balance, rotor blade motion and loading which is combined with noise prediction code ANOPP2 [8]. Also American FRAME (Fundamental Rotorcraft Acoustic Modeling from Experiments) [9] can be mentioned.

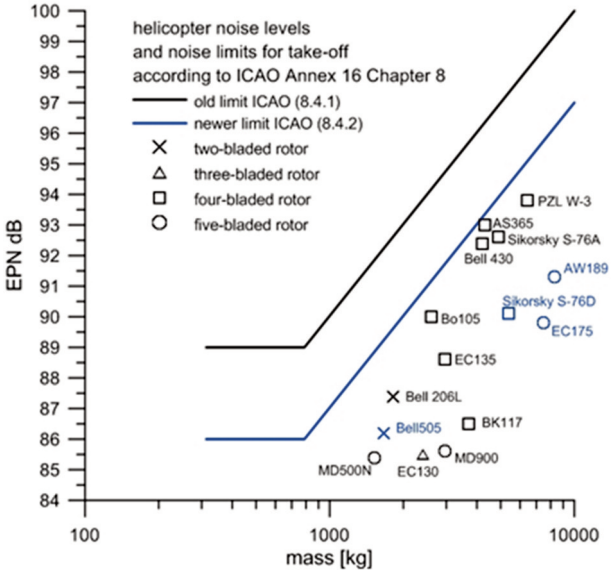

Fig. 1. Level of noise generated by helicopters and limits ICAO for phase of take-off.

Objectives of the European programs Friendcopter [10] and Green RotorCraft (GRC) – a component of the Clean Sky initiative were to reduce helicopter noise footprint area and reduce the noise perceived on ground. Development of new blades of Blue EdgeTM concept [11], [12] was concentrated on reduction of noise generated by blade vortex interaction (BVI). The five-bladed main rotor with blade tip speed decreased to 180m/s was applied at the Bluecopter demonstrator helicopter to accomplish further noise reduction [13]. Besides diminished noise level the additional effects of variable rotor speed were analyzed due to helicopter performance improvement [14], [15], [16]. It is worth to notice that noise reduction effectiveness of increased number of rotor blades combined with slower blade tip speed were in the past practically confirmed in the case of quieter version of the Hughes OH-6 [17] and in the case of Whisper Jet modification of the Sikorsky S-55 helicopter [18].

The paper presents results of calculations of performance and rotor loads for versions of light helicopter with different number of rotor blades and different blade tip speed. For the simulation calculations two models of the main rotor were applied. In the case of computing the helicopter balance and power required for flight the simplified model consisted of stiff fuselage with attached aerodynamic characteristics and main rotor treated as a disk area with averaged value of induced velocity and aerodynamic coefficients. For chosen flight states the more precise model of elastic blade was applied to calculate components of rotor loads and blade deflections. Changes of rotor noise level generated in hover due to number of blades and its tip speed were estimated applying Davidson-Hargest formula [19]. Results of simulation indicate effectiveness of lowered blade tip speed for reduction helicopter noise and simultaneously increased number of rotor blades allows to preserve helicopter performance on acceptable level.

2. HELICOPTER MODEL

For calculation the helicopter balance conditions and power required for flight as function of speed the simplified helicopter model is applied which includes stiff rotor disk and fuselage with assigned aerodynamics characteristics. For given speed of helicopter the balance conditions are met if in the next step of iteration process the angles of helicopter pitching and rolling differ less than 0.1°. For determined equilibrium forces of main rotor and tail rotor the corresponding deflections of swashplate and pitch of tail rotor blades are defined. Scheme of helicopter loads and geometrical data applied for longitudinal balance are shown in Fig. 2.

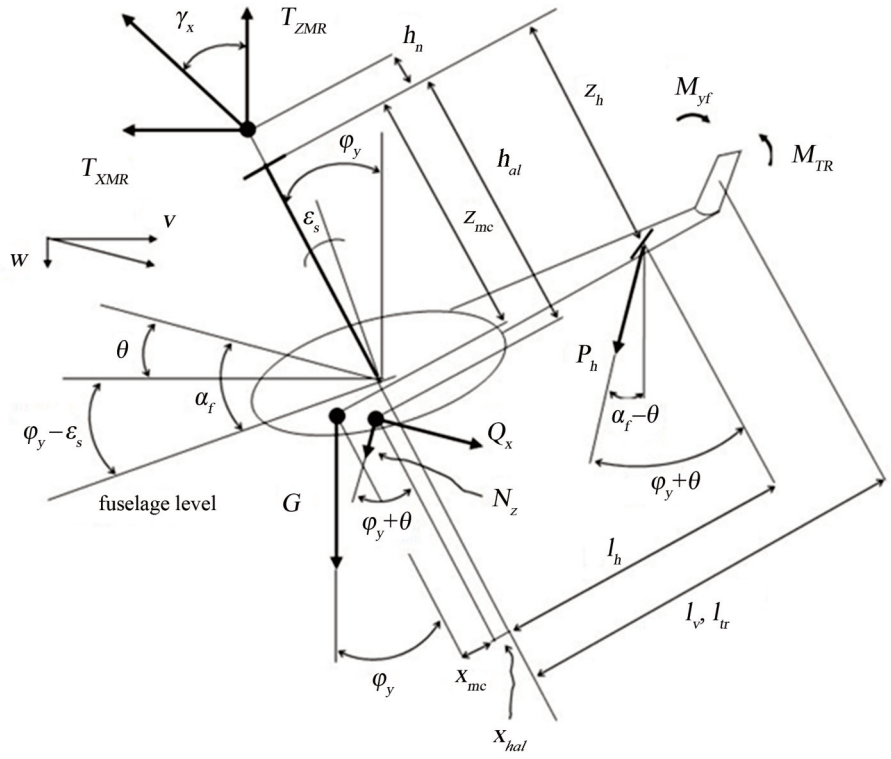

Fig. 2. Scheme of helicopter geometry and loads in longitudinal plane.

Notation of parameters shown in Fig. 2 is as follows:
w, v – components of flight speed,
θ – flight path angle, where θ = arc tg (w/v),
φ_y – pitch angle of rotor shaft,
ε_s – built-in angle of rotor shaft axis due to fuselage vertical,
α_f – fuselage angle of attack,
T_{XMR}, T_{ZMR} – components of main rotor thrust,
G – helicopter weight,
Q_x – fuselage drag,
N_z – lift of fuselage,
P_h – lift of horizontal stabilizer,

M_{yf} – aerodynamic moment of fuselage,
M_{TR} – moment of tail rotor,
x_{mc}, z_{mc} – location of helicopter mass center due to rotor hub center,
h_n – height over rotor hub of suspension point for helicopter treated as physical pendulum,
h_{a1}, x_{ha1} – location of fuselage aerodynamic forces due to rotor hub center,
l_h, l_v, l_{tr} – distances of horizontal stabilizer, fin, axis of tail rotor due to main rotor axis,
z_h – height of main rotor hub over horizontal stabilizer.

For given helicopter flight speed and fuselage angle of attack α_f fuselage lift force N_z drag force Q_x can be defined:

$$Q_x = \frac{1}{2}\rho \cdot \left(v^2 + w^2\right) \cdot \pi R_{MR}^2 \cdot c_{xf}\left(\alpha_f\right) , \tag{1}$$

$$N_z = \frac{1}{2}\rho \cdot \left(v^2 + w^2\right) \cdot \pi R_{MR}^2 \cdot c_{zf}\left(\alpha_f\right) , \tag{2}$$

where
ρ – density of air,
$c_{xf}\left(\alpha_f\right), c_{zf}\left(\alpha_f\right)$ – fuselage drag and lift coefficients,
R_{MR} – main rotor radius.

The components of main rotor thrust are determined using force equilibrium conditions:

$$T_{XMR} = Q_x \cos\left(\alpha_f - \theta\right) - N_z \sin\left(\alpha_f - \theta\right) - P_h \sin\left(\alpha_f - \theta\right) , \tag{3}$$

$$T_{ZMR} = Q_x \sin\left(\alpha_f - \theta\right) + N_z \cos\left(\alpha_f - \theta\right) + P_h \cos\left(\alpha_f - \theta\right) + G \tag{4}$$

Fuselage pitch angle is calculated applying equation of moments defined due to suspension point of helicopter treated as physical pendulum:

$$\begin{aligned} &G\left(h_n + z_{mc}\right)\sin\phi_y - Gx_{mc}\cos\phi_y - P_h l_h \cos\left(\phi_y + \theta\right) + P_h\left(h_n + z_h\right)\sin\left(\phi_y + \theta\right) \\ &+N_z\left(h_n + h_{a1}\right)\sin\left(\phi_y + \theta\right) - N_z x_{ha1}\cos\left(\phi_y + \theta\right) - Q_x\left(h_n + h_{a1}\right)\cos\left(\phi_y + \theta\right) \\ &-Q_x x_{ha1}\sin\left(\phi_y + \theta\right) + M_{yf} + M_{TR} = 0 \end{aligned} \tag{5}$$

height of suspension point over rotor hub is as follows:

$$h_n = \frac{k_{MR} \cdot S_{hh} \cdot \left(\Omega R_{MR}\right)^2 \cdot l_{hh}}{2 \cdot T \cdot R_{MR}^2} , \tag{6}$$

where
l_{hh} – distance of flapping hinge measured from rotor shaft axis,
S_{hh} – static mass moment of blade about flapping hinge,
k_{MR} – number of rotor blades,
R_{MR} – radius of rotor blade,
Ω – rotational speed of main rotor,
T – main rotor thrust.

Taking into account dimensionless coefficients μ_o rotor advance ratio and λ_o rotor inflow ratio, the value of rotor blade collective pitch ϑ_o can be determined:

$$\vartheta_o = \frac{c_T^* + \vartheta_s \left(t_4 + 0,5\mu_o^2 t_2\right) + \lambda_o \left(t_2 + 2\mu_o^2\right)}{t_3 + 0,5\mu_o^2 t_1} \quad , \tag{7}$$

where

c_T^* – main rotor thrust coefficient,

ϑ_s – geometric twist of rotor blade,

t_1 , t_2 , t_3 , t_4 – constants depend on tapered shape of rotor blade defined as follows:

$$t_n = 4\int_{\bar{r}_1}^{\bar{r}_2} \frac{b}{b_o} \bar{r}^{(n-1)} d\bar{r} \quad , \tag{8}$$

where

$\bar{r}_1$, $\bar{r}_2$ – relative radius, aerodynamic non-active at root and tip of rotor blade,

b_o – theoretical chord of rotor blade in the middle of rotor hub,
b – current chord of rotor blade.

Following equation defines main rotor thrust coefficient c_T^*:

$$c_T^* = \frac{8\,T}{\rho\,\Omega^2 R_{MR}^3\, a\, k_{MR} b_{07}} \quad , \tag{9}$$

where

$a = dc_z/d\alpha$ – airfoil lift curve slope,

b_{07} – chord rotor blade at radius r = 0,7R_{MR}.

Rotor blade flapping coefficients a_o – angle of rotor cone, a_1 – rotor longitudinal tilt and b_1 – rotor lateral tilt can be found applying blade collective pitch ϑ_o and coefficients μ_o rotor advance ratio, λ_o rotor inflow ratio:

$$a_o = \frac{\left(t_4 + 0,5\,\mu_o^2 t_2\right)\vartheta_o - \left(t_5 + 0,5\,\mu_o^2 t_3\right)\vartheta_s - t_3\lambda_o}{\gamma^*} \quad , \tag{10}$$

where characteristic of rotor blade (Lock number) is equal:

$$\gamma^* = \frac{8\,I_{hh}}{\rho\, R_{MR}^4 a\, b_{07}} \quad , \tag{11}$$

I_{hh} – blade mass moment of inertia about flapping hinge

$$a_1 = \frac{\mu_o \left(2\,t_3\vartheta_o - 2\,t_4\vartheta_s - \lambda_o t_2\right)}{t_4 - 0,25\,\mu_o^2 t_2} \quad , \tag{12}$$

$$b_1 = \frac{\mu_o t_3 a_o + t_4 K \bar{v}}{t_4 + 0,25\mu_o^2 t_2} \ , \tag{13}$$

where $\bar{v}$ – relative induced velocity

$$\bar{v} = \frac{v_i}{\Omega R_{MR}} \ , \tag{14}$$

K – coefficient of induced velocity distribution at rotor disk:

$$K = \frac{4\mu_o}{3\left(1,2\lambda_o + \mu_o\right)} \ . \tag{15}$$

Introducing blade flap-pitch coefficient k_{fp}, corrected values of blade flapping coefficients a_{1y}, b_{1y} about plane of deflected swashplate can be defined:

$$a_{1y} = \frac{a_1 + \bar{k}_{fp} b_1}{1 + \bar{k}_{fp}^2} \ , \tag{16}$$

$$b_{1y} = \frac{b_1 - \bar{k}_{fp} a_1}{1 + \bar{k}_{fp}^2} \ , \tag{17}$$

Swashplate deflection angles θ_{tx} and θ_{ty} about axis of rotor shaft can be determined taking into account blade flapping coefficients a_{1y}, b_{1y} and parameters of helicopter balance – tail rotor thrust T_{TR}, main rotor thrust T_{MR} and angle of helicopter rolling φ_x and pitching φ_y:

– swashplate pitching angle

$$\theta_{ty} = \frac{\left(a_{1y} - \phi_y + \gamma_x\right) D_1 - \left(\phi_x - T_{TR}/T_{MR} - b_{1y}\right)}{D_1^2 + D_2^2} \ , \tag{18}$$

– swashplate rolling angle

$$\theta_{tx} = \frac{b_{1y} - \phi_x + T_{TR}/T_{MR} - D_2\theta_{ty}}{D_1} \ , \tag{19}$$

where D_1, D_2 – geometrical coefficients of control blade pitch system.

For defined helicopter balance at chosen flight speed, demanded components of rotor forces and known position of rotor shaft axis the more exact model of flexible blades can be applied to calculate blade loads distributions with mutual effects of their deformations which are changing due to blade azimuthal position on rotor disk.

The model of the main rotor, for each blade and hub arm, consists of lumped masses set attached to elastic axis. The physical model of one rotor blade is shown in Fig. 3.

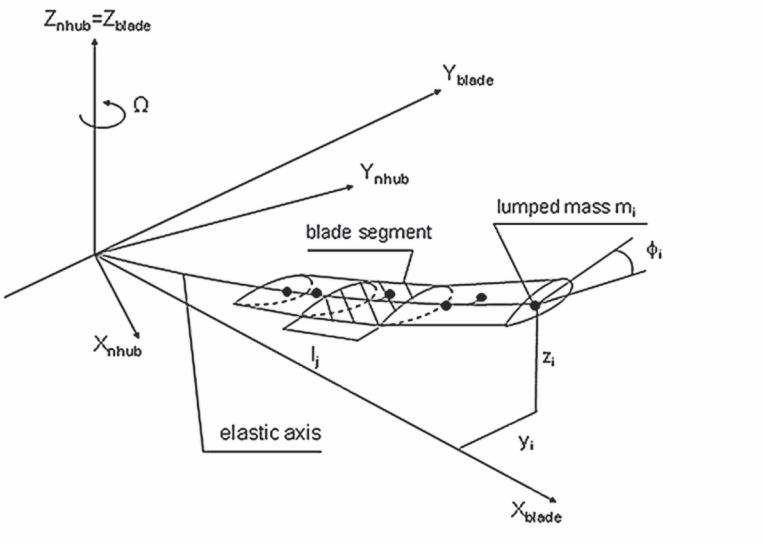

Fig. 3. Model of rotor blade with lumped masses distributed along elastic axis.

The following assumptions are applied to define blade model:

- mass distribution of the real blade is replaced by set of lumped masses which represent inertial features of blade segments,
- lumped masses are located at the gravity centers of blade segments,
- sections of elastic axis connect lumped masses,
- elastic axis represents blade torsion, in-plane and out-of-plane bending stiffness of in thrust and revolution planes,
- blade is articulated to rotor hub allowing flap, lead-lag and pitch motion of blade,
- blade dampers are attached to limit blade lead-lag motion,
- in non-deformed state the blade elastic axis is coincident with the blade pitch axis.

The simulation algorithm allows for multi-blade analysis in which motion and loads of each blade are calculated for their individual azimuthal position on rotor disk. For applied time step, forces coming from all blades create temporary resultant loads of the main rotor hub. Repeating computation cycles yields the time-runs of rotor loads and blade deflections.

The calculation model consists of equations of motion for flexible rotor blades which include effects of torsion deflections as well in-plane and out-of-plane bending of blade elastic axes.

The equations of rotor blades motion are solved using Runge-Kutta method. In the case of blades according to the Galerkin method, the motion parameters are assumed as a combination of shares of the considered eigen modes of the rotor blades. The deflections of the blade elastic axis *y, z, φ* are equal to superposition of modal components:

$$y(x,t)=\sum_{i1=1}^{I1}\rho_{i1}(t)y_{i1}(x);\quad z(x,t)=\sum_{i2=1}^{I2}\delta_{i2}(t)z_{i2}(x);\quad \varphi(x,t)=\sum_{i3=1}^{I3}\eta_{i3}(t)\varphi_{i3}(x), \tag{20}$$

where

$y_{i1}, z_{i2}, \varphi_{i3}$ – eigen modes of in-plane, out-of-plane bending and torsion respectively,
$\rho_{i1}, \delta_{i2}, \eta_{i3}$ – time dependent shares of eigen modes, which are determined in computing process,
$I1, I2, I3$ – numbers of considered bending and torsion eigen modes.

Applying formulas (20), the equations of blade motion can be transformed into sets of equations (21) related to each considered blade eigen mode:

$$\ddot{\rho}_{i1} + \rho_{i1} p_{i1}^2 = Q_{Y_{i1}} \qquad i1 = 1,\ldots,I1 \ , \tag{21a}$$

$$\ddot{\delta}_{i2} + \delta_{i2} f_{i2}^2 = Q_{Z_{i2}} \qquad i2 = 1,\ldots,I2 \ , \tag{21b}$$

$$\ddot{\eta}_{i3} + \eta_{i3} \nu_{i3}^2 = Q_{\phi_{i3}} \qquad i3 = 1,\ldots,I3 \ , \tag{21c}$$

where

p_{i1}^2 , f_{i2}^2 , ν_{i3}^2 – square of eigen mode frequencies for bending in-plane, out-of-plane and torsion,

$Q_{Y_{i1}}, Q_{Z_{i2}}, Q_{\varphi_{i3}}$ – generalized forces for considered eigen modes of the rotor blade.

Aerodynamic forces acting on segment of blade at given azimuth position on the rotor disk are computed applying the blade element theory. The local angle of attack at blade cross-section depends on control of pitch angle and on temporary conditions of airflow:

$$\alpha = \phi_{coll} + \phi_{x\_cycl} \cos\Omega t + \phi_{y\_cycl} \sin\Omega t + \vartheta_s + \Delta\phi - \kappa_{fp}\beta - arc\,tg\left(\frac{u_Z}{u_X}\right), \tag{22}$$

where

ϕ_{coll} – blade collective control angle,

ϕ_{x_cycl} , ϕ_{y_cycl} – cyclic control angle due to roll and pitch deflections of the swash-plate,

ϑ_s – geometric twist,

$\Delta\varphi$ – torsion deformation,

κ_{fp} – coefficient of coupling flap and blade pitch,

β – blade flap angle at horizontal hinge of rotor head,

u_z, u_x – components of the cross-section airflow of rotor blade: out-of-plane and in-plane.

3. SIMULATION RESULTS

Simulation calculation concerning helicopter performance, rotor loads and blade deformations were performed for data of hypothetical helicopter. The main rotor radius was assumed to be equal 3.75m. Formula defined by Davidson and Hargest was applied to estimate level of noise generated by helicopter in hover at 150m above the ground:

$$\mathrm{SPL150} = 10\log\left[\left(\Omega R_{MR}\right)^6 \cdot A_b \left(c_t/\sigma\right)^2\right] - 36.7\,[\mathrm{dB}], \tag{23}$$

where:

- c_t – thrust coefficient applied for SPL150 calculation

$$c_t = \frac{T_{MR}}{\rho \cdot \pi\, R_{MR}^2 \cdot \left(\Omega\, R_{MR}\right)^2} \ , \tag{24}$$

- T_{MR} – rotor thrust, [N]

- ρ – air density, [kg/m^3]
- R_{MR} – rotor radius, [m]
- ΩR_{MR} – blade tip speed, [m/s]
- A_b – summary area of rotor blades, [m^2]
- σ – ratio of blade area to rotor disk area, $\sigma = k_{MR}\, b/\pi/R_{MR}$
- k_{MR} – number of blades,
- b – blade chord. [m]

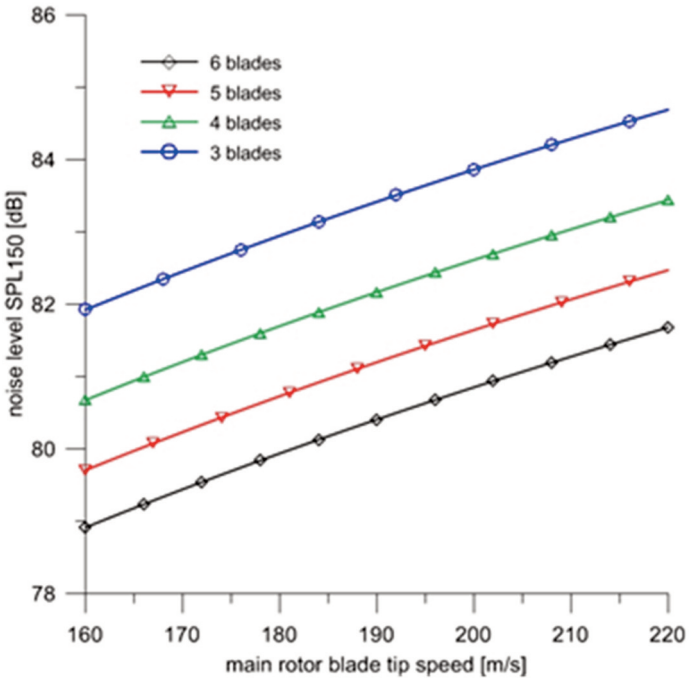

Fig. 4. Changes of rotor noise level generated in hover due to number of rotor blades and blade tip speed

For helicopter of mass equal 1,000kg, variants of main rotor with different number of blades from three to six and blade tip speed varying from 160m/s to 220m/s were considered. According to Eqs. 23, results of calculation the sound pressure level beneath the rotor hub are shown in Fig. 4. It can be noticed that the lowest sound level equal 79dB is generated by a six-bladed rotor for the lowest assumed blade tip speed of 160m/s. The highest sound level over 84dB would be observed in the case of three-bladed rotor with blade tip speed of 220m/s. Reduction of blade tip speed to 160m/s for three-bladed rotor allows to reach diminished sound level of 82dB. The sound levels calculated according to Davidson and Hargest formula for some commercial heavier helicopters and variants of hypothetical light helicopter are compared in Fig. 5. Low speed of blade tip and increased number of rotor blades can result in considerable reduction of helicopter noise level. Following designations are introduced to mark variants of hypothetical light helicopter which are shown in Fig. 5:

– ILX27-L3V220 – three-bladed rotor, blade tip speed 220 m/s, helicopter mass 1.000 kg
– ILX27-L3V160 – three-bladed rotor, blade tip speed 160 m/s, helicopter mass 1.000 kg
– ILX27-L6V160 – six-bladed rotor, blade tip speed 160 m/s, helicopter mass 1.000 kg
– ILX27-L6V160mass1500 – six-bladed rotor, blade tip speed 160 m/s, helicopter mass 1.500 kg

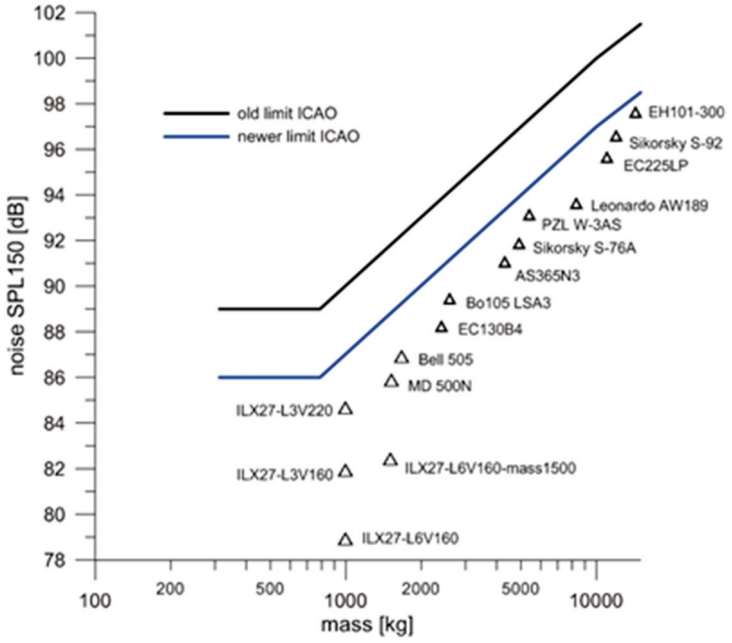

Fig. 5. Comparison of helicopter noise level estimated for hover at 150m above the ground.

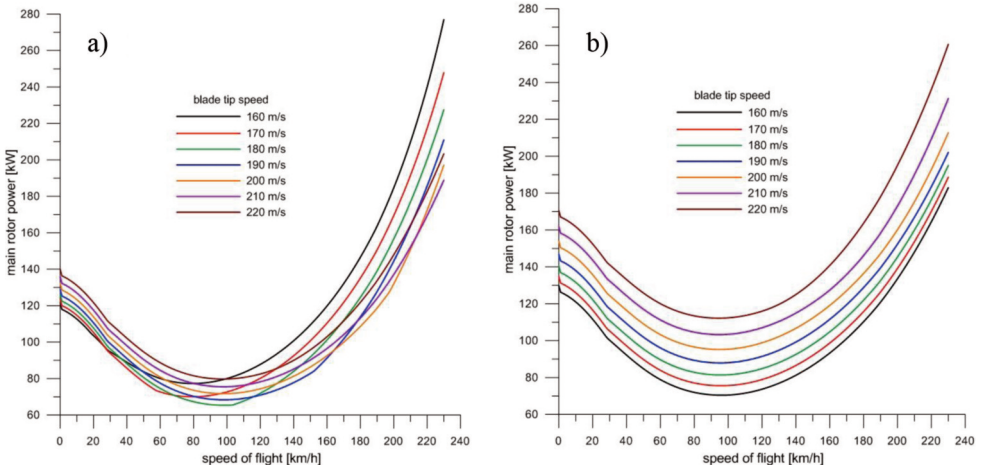

Fig. 6. Comparison of power required to drive the main rotor due to flight speed and rotor blade tip speed for helicopter mass m=900 kg: a) three-bladed rotor, b) six-bladed rotor.

Influence of blade tip speed on helicopter performance can be noticed in Fig. 6 showing power required to drive main rotor due to flight speed for helicopter mass of 900kg with three-bladed and six-bladed rotor variants. Blades of the same geometry were applied for both versions of main rotor. Plots of corresponding power required to drive five-bladed tail rotor, the same for each case of main rotor, are collected in Fig. 7. Power required to drive the three-bladed variant of main rotor (Fig. 6a) in hover condition reaches the lowest value for the lowest considered blade tip speed of 160m/s which is also acceptable due to low level of generated noise. But for speed of helicopter close to economical condition in range of 90÷110km/h the lowest value of main rotor power is observed for higher blade tip speed of 180÷190m/s range.

The three-bladed rotor of quiet helicopter with blade tip speed of 160m/s requires nearly 15kW more power at economical flight speed than rotor with higher blade tip speed. For larger flight speed the power required for quiet three-bladed rotor (160m/s tip speed) quickly raises reaching 240kW at flight speed of 220km/h compared to required power of 180kW for rotor variant with blade tip speed of 200÷210m/s.

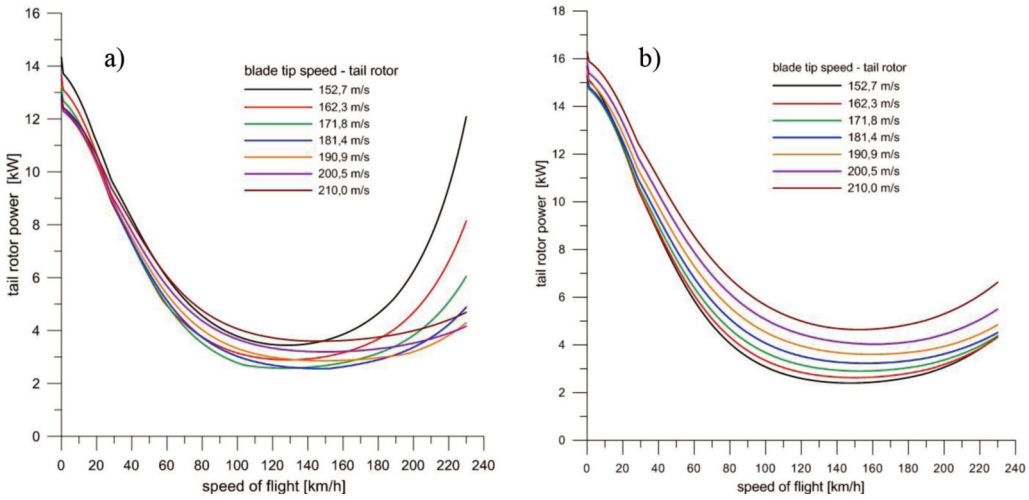

Fig. 7. Power required to drive five-bladed tail rotor for 900 kg mass helicopter due to flight speed and tail rotor blade tip speed: a) helicopter with three-bladed main rotor, b) helicopter with six-bladed main rotor.

Among six-bladed rotors the lowest values of required power are achieved in the whole range of helicopter flight speed from hover to high speed conditions for rotor variant with quiet blade tip speed of 160m/s (Fig. 6b). The higher values of power required to drive the three-bladed rotor can be explain as result of applying greater angles of blade collective pitch to create demanded lift force and as consequences the earlier appearance of compressibility effects for advancing blade and effects of separated airflow for retreating blade. Increased power of three-bladed rotor version generates greater reaction moment which has to be compensated by higher tail rotor thrust, also with higher value of power required to drive tail rotor (Fig. 7a). In the case of quiet six-bladed main rotor (blade tip at 160m/s), power required to drive tail rotor is kept at the lowest level in all considered flight speed of helicopter (Fig. 7b).

Range of changes of power required to drive main rotor is better presented in Fig. 8a in which are shown plots of power for three- and six-bladed rotor with the lowest 160m/s and highest 220m/s blade tip speed for helicopter mass of 900kg compared to plot of power of six-bladed rotor (blade tip 220m/s) for overloaded helicopter of 1.400kg take-off mass. It is worth to notice an advantage of applying rotor with increased number of blades. Power of main three-bladed quiet rotor (blade tip speed ΩR_{MR}=160m/s) for helicopter take-off mass of 900kg at high speed flight (220km/h) reaches nearly the same value as power of six-bladed rotor with blade tip speed equal 220m/s for helicopter with greater mass of 1.400kg. In the case of regulated rotor rotational speed additional feature of six-bladed rotor can be revealed. At low blade tip speed for standard helicopter take-off mass quiet rotor will generate low level noise, but in the urgent case at increased blade tip speed operation of overloaded helicopter would be possible.

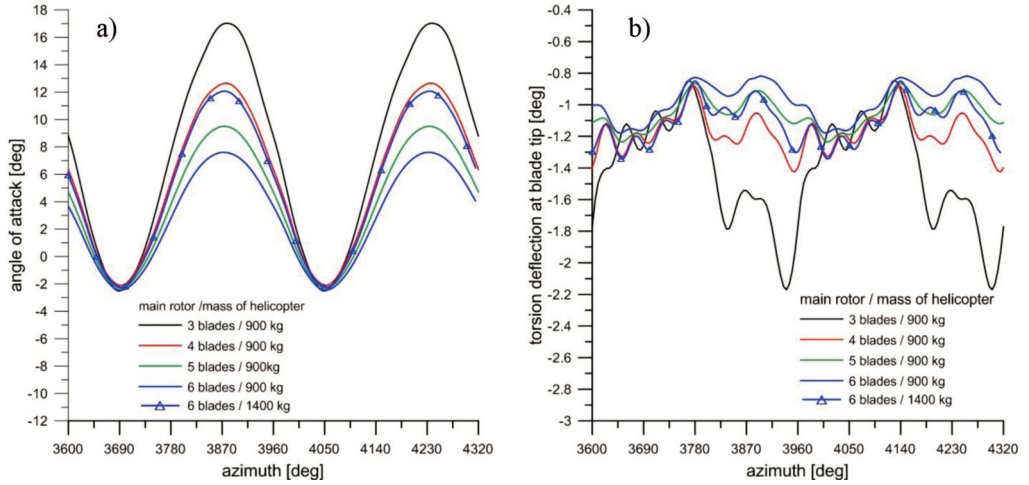

Fig. 8. Range of change of power required to drive main rotor and collective pitch change for mass helicopter 900 kg and 1.400 kg due to flight speed and rotor blade tip speed: a) rotor required power, b) collective pitch of main rotor blades.

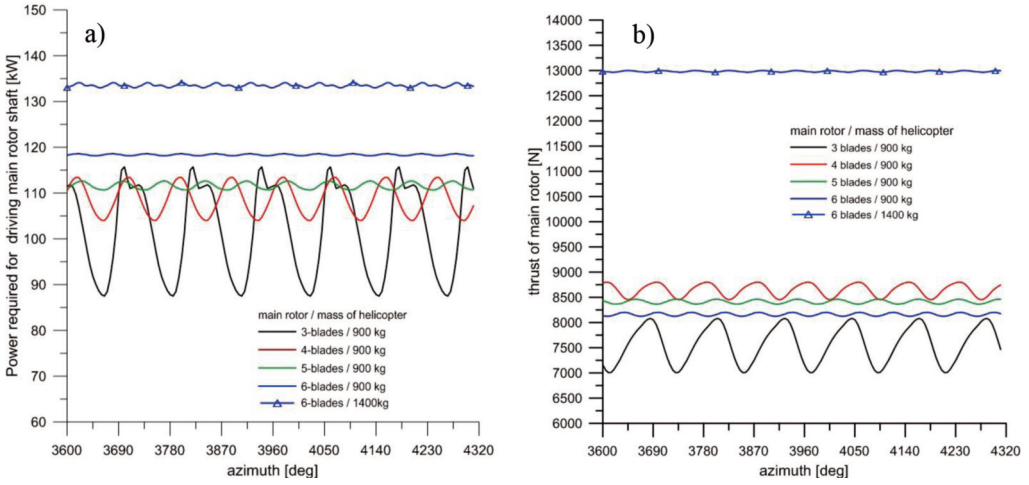

Fig. 9. Power required to drive main rotor and rotor thrust during rotor revolution in level flight at velocity of 190km/h due to number of rotor blades, blade tip speed 160m/s, helicopter mass 900kg and 1.400kg (only six-bladed rotor): a) power required, b) rotor thrust. Simulation solution for 11th and 12th rotor revolution.

Introducing a more complex model of elastic rotor blade allows to calculate changes of rotor hub loads and blade deflections due to azimuthal blade position for applied variants of rotor with different number of blades (Fig. 9÷11). Calculation for all versions of rotors were performed for quiet variant with minimum value of considered blade tip speed equal 160m/s. Mass of 900kg was applied for helicopters with three-, four-, five- and six-bladed rotors and six-bladed case of overloaded helicopter with mass of 1.400kg was assumed. Simulation calculations were executed for time corresponding to twelve rotor revolutions. Results for the last two rotor revolutions are shown in Fig. 9÷11. For chosen conditions of level flight at speed of 190km/h following plots are presented:

– power required for driving main rotor shaft (Fig. 9a),

– thrust of main rotor (Fig. 9b),

– blade pitch control moment (Fig. 10a),
– control force of rotor blades collective pitch (Fig. 10b),
– angle of attack at blade tip (Fig. 11a),
– torsion deflection of rotor blade at tip section (Fig. 11b).

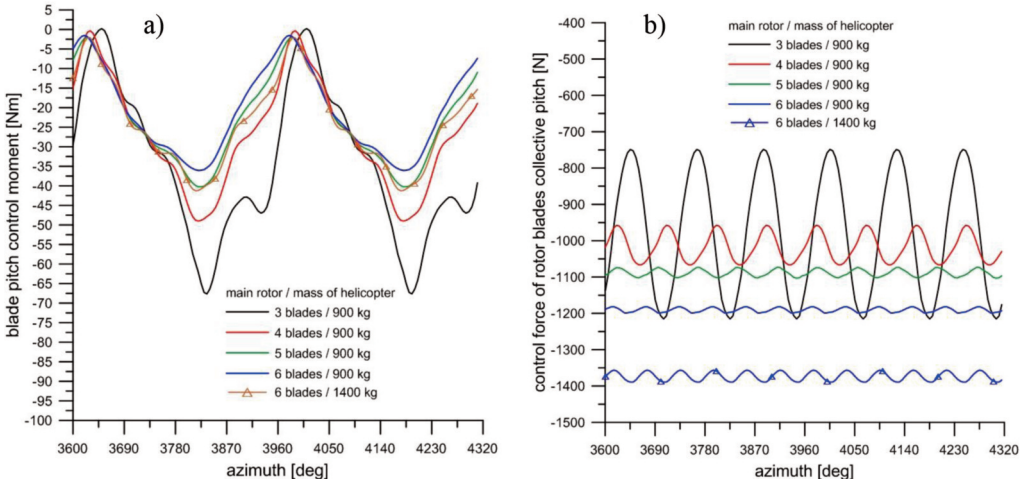

Fig. 10. Changes of pitch control moment of main rotor blade (a) and control force of collective pitch of all main rotor blades (b) as function of azimuth position in level flight conditions at speed v=190 km/h, main rotor blade tip speed 160m/s, rotor variants: three, four, five and six blades for helicopter mass of 900 kg, for helicopter mass of 1.400 kg only six-bladed rotor, simulation solution for 11th and 12th rotor revolution.

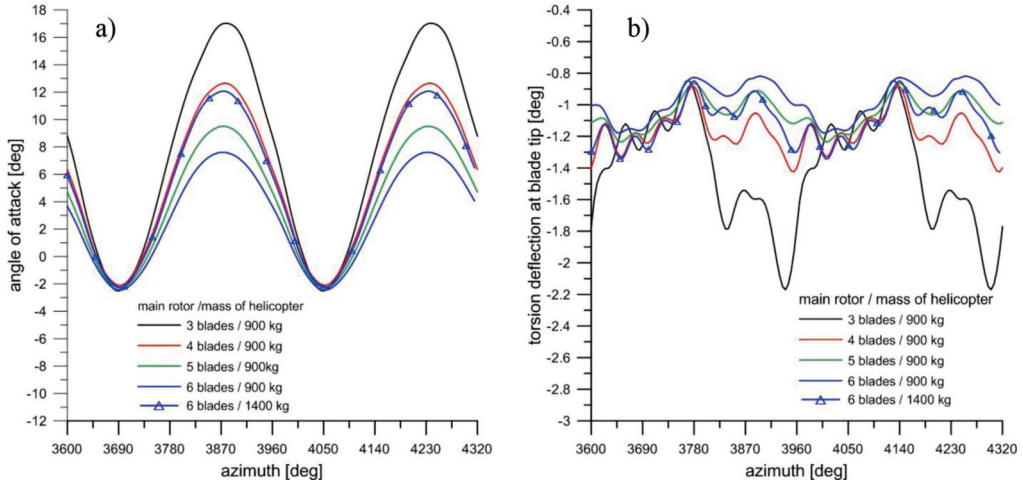

Fig. 11. Angle of attack at tip of rotor blade (a) and torsion deflection of rotor blade at tip section (b) as function of blade azimuth position in level flight conditions at speed v=190km/h, main rotor blade tip speed 160m/s, rotor variants: three, four, five and six blades for helicopter mass of 900 kg, for helicopter mass of 1.400 kg only six-bladed rotor, simulation solution for 11th and 12th rotor revolution.

Time plots of power required to drive main rotor (Fig. 9a) and plots of rotor thrust (Fig. 9b) show that the lowest oscillations during rotor revolution can be achieved for six-bladed rotor. Even in the case of six-bladed overloaded helicopter with mass of 1.400kg the oscillations of power and rotor thrust are

considerable lower than for helicopter of mass of 900kg but with lesser number of rotor blades. The excessive oscillations of power and rotor thrust, especially for three-bladed rotor, can be associated with appearance of flow separation zone for tip sections of blade at vicinity of its retreating azimuthal position on rotor disk, as it can be noticed in Fig. 13a. Increased number of blades causes higher frequencies of power and rotor thrust oscillations but with remarkable reduction of their amplitudes.

For the three-bladed rotor rapid changes of blade aerodynamic loads during crossing borders of flow separation zone generate large moments and forces at elements of blade pitch control system (Fig. 10). Increased number of rotor blades allow to achieve demanded value of rotor thrust at relatively lower collective and cyclic pitch and lower angle of attack at blade sections (Fig. 11a). Comparing plots of blade torsion deflections (Fig. 11b) the effects of lack of separation flow zones for increased number of rotor blades can be noticed. In the case of three-bladed rotor the torsion deflection of blade tip reaches value of -2° while for the rotor with greater number of blades torsion deflection at blade tip is in range of -0.9° to 1.4° at the same flight sped of 190km/h.

More information on blade behavior can be found in plots of blade parameter distributions on rotor disk. In Fig. 12÷15 disk distributions for following parameters are collected: blade angle of attack, difference of critical angle and local angle of attack, blade torsion deflections and blade out-of-plane deflection. Disk distributions concern the cases of three-bladed and six-bladed helicopter of 900kg mass and version of six-bladed helicopter of 1.400kg mass. In level flight conditions at speed of 190km/h with assumed blade tip speed equal to 160m/s the positive features of six-bladed rotor, even for overloaded helicopter of 1.400kg mass can be noticed.

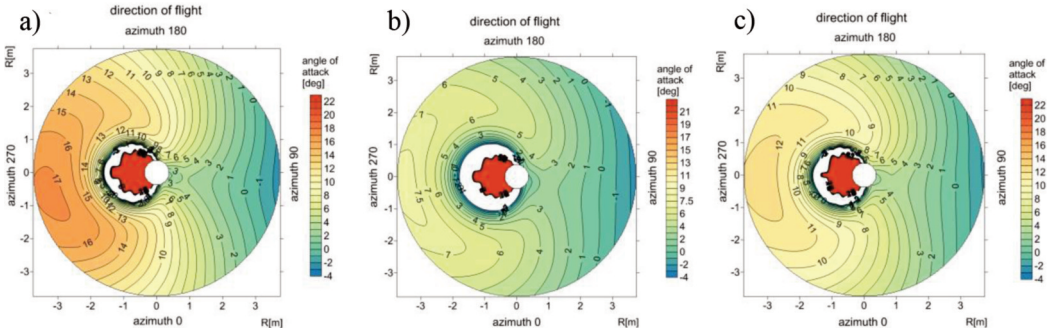

Fig. 12. Rotor disk distribution of blade angle of attack in level flight at speed 190km/h with blade tip speed 160m/s: a) three-bladed rotor, helicopter mass 900 kg; b) six-bladed rotor, helicopter mass 900kg; c) six-bladed rotor, helicopter mass 1.400kg.

For helicopter of 900kg mass with three-bladed rotor for retreating blade at 270° azimuthal position the local angle of attack reaches 17° at blade tip sections (Fig. 12a). For the same flight condition in the case of 900kg mass helicopter but with six-bladed rotor, the angle of attack for blade azimuthal position close to 270° reaches only 7.5° (Fig. 12b). The lower values of angles of attack for six-bladed rotor at retreating blade positions allow to preserve appearance of separated airflow zone (Fig. 13a, b). The lack of excessive high angles of attack in vicinity of retreating blade positions and lack of separated airflow zone is also noticed in the case of overloaded helicopter of 1.400kg mass with six-bladed rotor (Fig. 12c, Fig. 13c).

In the case of three-bladed rotor crossing the border of separated airflow zone causes increased level of blade torsion deflection reaching value of -2.2° for blade tip at azimuthal position of 330° (Fig. 14a). Oscillations of torsion deflection with frequency corresponding to the blade torsion eigen mode is observed even at azimuthal position outside zone of separation flow. Blade torsion deflections of

six-bladed rotor are significantly lower (Fig. 14b, Fig. 14c). Similarly lower out-of-plane deflections of blades are observed for six-bladed rotors (Fig. 15b, Fig. 15c) than in the case of three-bladed rotor (Fig. 15a).

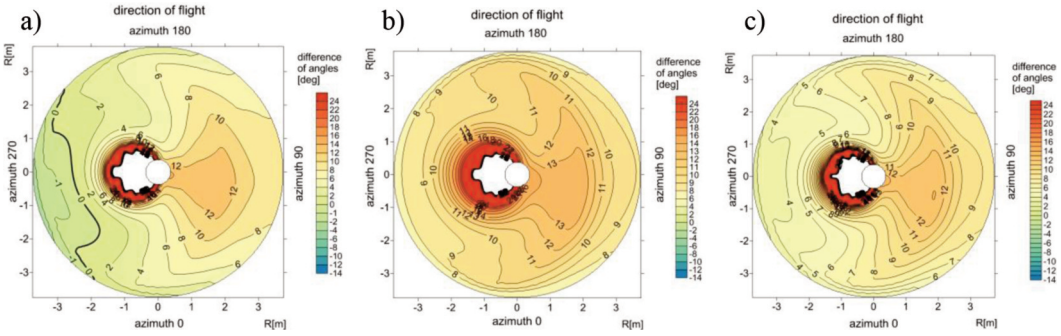

Fig. 13. Rotor disk distribution of difference of critical and local blade angle of attack in level flight at speed 190km/h with blade tip speed 160m/s: a) three-bladed rotor, helicopter mass 900kg; b) six-bladed rotor, helicopter mass 900kg; c) six-bladed rotor, helicopter mass 1.400kg.

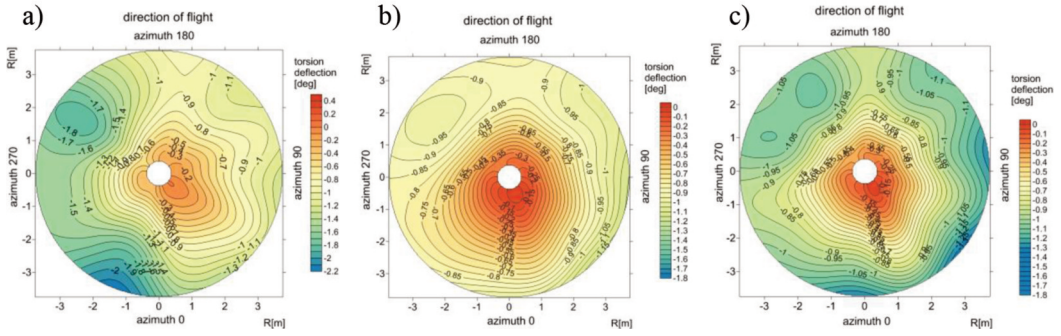

Fig. 14. Rotor disk distribution of blade torsion deflection in level flight at speed 190km/h with blade tip speed 160m/s: a) three-bladed rotor, helicopter mass 900kg; b) six-bladed rotor, helicopter mass 900kg; c) six-bladed rotor, helicopter mass1.400kg.

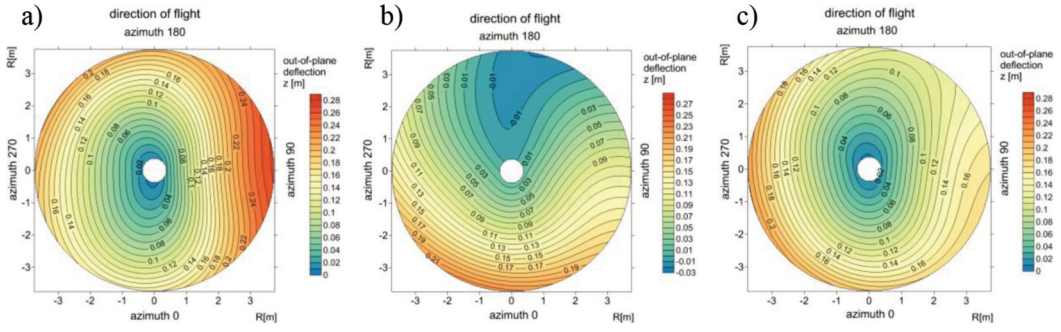

Fig. 15. Rotor disk distribution of blade out-of-plane deflection in level flight at speed 190km/h with blade tip speed 160m/s: a) three-bladed rotor, helicopter mass 900kg; b) six-bladed rotor, helicopter mass 900kg; c) six-bladed rotor, helicopter mass1.400kg.

4. CONCLUSIONS

Results of calculations confirm some advantages of quiet helicopter with increased number of rotor blades. Generations of high value rotor thrust with preserved limits of helicopter low noise is possible in the case of introduction the rotor of increased number of blades and decreased blade tip speed. Increased number of blades allows to keep airflow conditions, even at high speed flight, without appearance a separation zone. Additionally increased number of blades enables to achieve lower amplitudes of variable components of rotor loads.

REFERENCES

[1] https://eu.azcentral.com/story/news/local/arizona-environment/2017/09/29/grand-canyon-air-tours-conservationists-hear-noisy-helicopters-tribes-sees-economic-returns/588119001/ [access 2019-06-10]

[2] Moorman, R. W., 2015, "Noise in the Parks", Vertiflite, March/April, pp. 34-38.

[3] Hampson, M., 2014, "OEM Perspectives on Noise", Vertiflite, January/February, pp. 18-23.

[4] https://www.hlnug.de/fileadmin/dokumente/laerm/gesetze/flugverkehr/ICAO_Annex16_Volume1.pdf [access 2019-06-10]

[5] https:/easa.europa.eu/easa-and-you/environment/easa-certification-noise-levels [access 2019-06-12]

[6] Botre, M., Brentner, K. S., Horn, J. F. and Wachspress, D., 2019, "Validation of Helicopter Noise Prediction System with Flight Data", *Vertical Flight Society 75th Annual Forum & Technology Display*, Philadelphia, Pennsylvania, May 13-16.

[7] Watts, M. E., Greenwood, E. and Stephenson, J.H., 2016, „Measurement and Characterization of Helicopter Noise at Different Altitudes", *American Helicopter Society 72nd Annual Forum & Technology Display*, West Palm Beach, Florida, May 16-19.

[8] Boyd, D. D., Greenwood, E., Watts, M. E. and Lopes, L. V., 2017, "Examination of a Rotorcraft Noise Prediction Method and Comparison to Flight Test Data", NASA-TM-2017-219370, Langley Research Center, Hampton, Virginia.

[9] Greenwood, E., 2017, "Helicopter Flight Procedures for Community Noise Reduction", *American Helicopter Society 73rd Annual Forum & Technology Display*, Fort Worth, Texas, May 9-11.

[10] https://cordis.europa.eu/docs/publications/1247/124772131-6_en.pdf – Friendcopter Publishable Final Activity Report, 2009. [access 2019-10-01]

[11] Rauch, P., Gervais, M., Cranga, P., Baud, A., Hirsch, J-F., Walter, A. and Beaumier, P., 2011, "Blue Edge™: The Design, Development and Testing of a New Blade Concept", *American Helicopter Society 67th Annual Forum*, Virginia Beach, Virginia, May 3-5.

[12] Delrieux Y., 2014, "From design to flight testing: overview of rotorcraft acoustic research at Onera for industrial applications", Journal AerospaceLab, Issue 7, June 2014.

[13] https://www.theengineer.co.uk/airbus-helicopters-bluecopter-reduces-noise-and-fuel-consumption/ [access 2019-06-06]

[14] Han, D., Pastrikakis, V. and Barakos, G. N., 2016, "Helicopter performance improvement by variable rotor speed and variable blade twist", Aerospace Science and Technology, **54**, pp. 164-173.

[15] Stevens, M. A., Lewicki, D. G. and Handschuh, R. F., 2015, "Concepts for Multi-Speed Rotorcraft Drive System – Status of Design and Testing at NASA GRC", *American Helicopter Society 71st Annual Forum*, Virginia Beach, Virginia, May 5-7.

[16] Khoshlahjeh, M. and Gandhi, F., 2013, "Helicopter Rotor Performance Improvement with RPM Variation and Chord Extension Morphing", *American Helicopter Society 69th Annual Forum*, Phonix, Arizona, May 21-23.

[17] Ropelewski, R. R., 1971, "Army, Hughes Demonstrate OH-6 Modified into 'Quiet' Helicopter", Aviation Week & Space Technology, March 1, p. 15.
[18] "Whisper Jet to keep canyon quiet", 2000, Flight International, 1-7 February, p. 29.
[19] Johnson, W., 2013, „*Rotorcraft Aeromechanics*", New York, Cambridge University Press.

OSIĄGI CICHEGO ŚMIGŁOWCA

Abstrakt

Hałas generowany przez śmigłowce jest jednym z głównych problemów związanych z eksploatacją wiropłatów. Wymagania ograniczenia hałasu śmigłowców znalazły odzwierciedlenie w przepisach zakładających zmniejszenie hałasu wytwarzanego przez wiropłaty. Znaczącym źródłem hałasu generowanego przez śmigłowce są łopaty wirnika nośnego oraz śmigła ogonowego. Znaczące obniżenie hałasu może być uzyskane w wyniku zmniejszenia prędkości końcówek łopat wirnika i śmigła ogonowego. Zmniejszenie prędkości obrotowej łopat pociąga za sobą spadek wytwarzanego ciągu wirnika i zmniejszenie osiągów śmigłowca. Rozwiązaniem problemu może być zastosowanie większej liczby łopat wirnika. W pracy przedstawiono obliczeniowe wyniki dotyczące możliwych do uzyskania osiągów śmigłowca przy obniżonej prędkości obrotowej wirnika i zwiększonej liczbie łopat. Obliczenia przeprowadzono dla danych masowych hipotetycznego śmigłowca lekkiego. Wykonano symulacyjne obliczenia obciążeń wirnika i odkształceń łopat w kilku stanach lotu śmigłowca rozwiązując równania ruchu elastycznych łopat wirnika z zastosowaniem metody Galerkina przy uwzględnieniu wybranych postaci własnych łopat. Uwzględniono możliwość regulacji obrotów wirnika w zależności od stanu lotu. Przeprowadzone analizy mogą znaleźć zastosowanie przy określaniu parametrów wirnika cichego śmigłowca ze zmniejszoną prędkością wirnika dla obwiedni stanów lotu śmigłowca.

Słowa kluczowe: śmigłowiec, hałas, obciążenia wirnika.